

# Aggregation in Aqueous Poly(*N*-isopropylacrylamide)-*block*-poly(ethylene oxide) Solutions Studied by Fluorescence Spectroscopy and Light Scattering

Janne Virtanen,<sup>†</sup> Susanna Holappa,<sup>†</sup> Helge Lemmetyinen,<sup>‡</sup> and Heikki Tenhu<sup>\*,†</sup>

Laboratory of Polymer Chemistry, University of Helsinki, PB 55, FIN-00014 HY, Finland, and  
Institute of Materials Chemistry, Tampere University of Technology, PB 541,  
FIN-33101 Tampere, Finland

Received December 26, 2001; Revised Manuscript Received March 18, 2002

**ABSTRACT:** Block copolymers poly(*N*-isopropylacrylamide)-*block*-poly(ethylene oxide), PNIPA-*b*-PEO, were synthesized by free radical polymerization using macroazoinitiators bearing PEO chains with two different chain lengths ( $M_w = 550$  or  $1900$  g/mol). The molar mass of the PNIPA block varied from  $0.4 \times 10^5$  to  $7.3 \times 10^5$  g/mol. The cloud points of the aqueous copolymer solutions shifted to slightly higher temperatures only with the samples having the longer PEO block. Above the lower critical solution temperature (LCST) of PNIPA the block copolymers formed aggregates with a spherical core–shell structure sterically stabilized by a PEO shell. The formation and especially the shape of the aggregates were influenced by the length of the PNIPA block, the molar ratio of the repeating units of PNIPA and PEO, and the polymer concentration. A fluorescent probe 4-(dicyanomethylene)-2-methyl-6-(*p*-(dimethylamino)styryl)-4*H*-pyran, 4HP, was localized inside the polymer differently depending on the method of sample preparation. The microviscosity in the surroundings of the probe increased with the length of the PNIPA block. However, depending on the sample preparation method, the length of the PEO block was also observed to have an effect on the polarity of the environment around the probe. In general, increasing the block length of PEO affected critically the size and shape of the aggregates as well as the mass distribution within them above the LCST, owing to the enhanced solubilizing effect of PEO on the collapsing PNIPA and the improved steric stabilization of the aggregates induced by a PEO shell.

## Introduction

Amphiphilic block and graft copolymers are self-assembling materials which are capable of forming polymeric micelles in aqueous solutions.<sup>1</sup> The micelle formation is spontaneous if a part of the copolymer is hydrophobic and thus favors the buildup of a core–shell structure. However, in the case of hydrophilic copolymers an external stimulus affecting a part of the copolymer is required to induce the micelle formation.<sup>2–7</sup> Block and graft copolymers containing poly(ethylene oxide) (PEO) as a hydrophilic segment are widely synthesized and studied.<sup>8,9</sup> PEO is also often used for the stabilization of dispersions and emulsions. Amphiphilic copolymers containing PEO segments have been suggested to function as vehicles in drug delivery systems due to the biocompatibility of PEO.<sup>10</sup>

Polymers that respond to external chemical and physical stimuli like temperature, pH, ionic strength, solvent composition, electric field, and light have attracted a noticeable attention.<sup>11</sup> Poly(*N*-isopropylacrylamide) (PNIPA) is one of the most studied responsive polymers that exhibits a lower critical solution temperature (LCST) in water around 32 °C. This paper describes the syntheses of block copolymers, for which PNIPA was chosen as a hydrophobic block because of its thermosensitivity. For a hydrophilic block, poly(ethylene oxide) was chosen because of its high solubility in water in a wide temperature range, also above the LCST of PNIPA.

The synthetic methods for the preparation of well-defined diblock copolymers are widely being studied. Different homopolymers carrying specific functionalities as end groups may be connected with each other via the functional groups.<sup>12</sup> However, the yield of the diblock copolymer is often low due to the shielding of a functional group by a long polymer chain. Another method is to initiate the polymerization of a monomer with a reactive polymer, carrying either an ionic or radical moiety in the chain end. An example is the use of a redox system of a transition-metal ions such as  $\text{Ce}^{4+}$  and  $\text{Mn}^{3+}$  and a hydroxy-terminated polymer.<sup>2,13</sup> To prepare PNIPA-*b*-PEO copolymers, we have initiated the polymerization of NIPA by macroazoinitiators which contain PEO chains symmetrically at both ends of an AIBN derivative. This technique for the production of di- and triblock copolymers has been used in some cases.<sup>14</sup> Recently, much effort has been paid on new controlled radical polymerization techniques such as RAFT<sup>15</sup> and ATRP<sup>9</sup> to produce well-defined block copolymers as well.

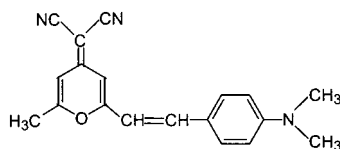
Owing to its high sensitivity, fluorescence spectroscopy is an ideal method to study dilute solutions of amphiphilic polymers. Especially, the formation of hydrophobic microdomains in water-soluble polymers may well be detected by incorporating fluorescent probes into the samples.<sup>16</sup>

Fluorescent donor–acceptor probes are sensitive to changes in both the polarity and the microviscosity of their surroundings.<sup>17</sup> The probe used in the present investigation is 4-(dicyanomethylene)-2-methyl-6-(*p*-(dimethylamino)styryl)-4*H*-pyran, 4HP, which exhibits intramolecular charge transfer (ICT) property and stereoisomerism. 4HP contains both electron donor and

<sup>†</sup> University of Helsinki.

<sup>‡</sup> Tampere University of Technology.

\* Corresponding author: tel +358-9-19150334; fax +358-9-19150330; e-mail Heikki.Tenhu@Helsinki.fi.

**Scheme 1. Structure of the Fluorescent Probe 4HP**

acceptor moieties being linked by an aromatic chromophore. Because both twisting and charge separation are involved in the formation of intramolecular charge transfer states, the fluorescence emission of 4HP is sensitive to both the solvent polarity and the microviscosity of the medium. The sensitivity of 4HP to local changes in its environment makes it possible to study the formation, structure, and stability of hydrophobic microdomains in a polymer system. The probe used in this study is only sparingly soluble in water but dissolves with the polymer, and thus it is likely to be found close to the hydrophobic domains of the aqueous polymer system.

Recently, we have prepared graft copolymers of PNIPA with a varying number of PEO grafts. We used fluorescence, EPR spectroscopy, and light scattering techniques in order to investigate the influence of the PEO grafts on the thermal behavior of a PNIPA in water.<sup>6</sup> It was concluded that the changes in the polarity and microviscosity in the surroundings of the fluorescent probe, 4HP, upon the collapse of PNIPA depended in general on the amount of PEO in the polymer, polymer concentration, and sample heating rate.

In this study, block copolymers with different chain lengths of PNIPA have been synthesized using two macroazoinitiators substituted with PEO of different chain lengths (MW 550 and 1900 g/mol). The thermal properties and aggregate formation of the block copolymers have been studied by static and dynamic light scattering and fluorescence spectroscopy. The purpose was to explore the effect of the length of PEO with respect to that of PNIPA on the formation of a core-shell nanostructures.

## Experimental Section

**Materials.** The monomer *N*-isopropylacrylamide (NIPA, Acros Organics) was purified by recrystallization in a benzene/*n*-hexane mixture and dried carefully in a vacuum. A known amount of poly(ethylene glycol) monomethyl ether ( $M_w$  550 g/mol; PEO<sub>550</sub>, Fluka and 1900 g/mol; PEO<sub>1900</sub>, PolySciences) was dissolved in dichloromethane (Riedel-de Haën), and the mixture was dried over molecular sieves 3 Å (Riedel-de Haën) before use. 4,4'-Azobis(4-cyanopentanoic acid) (ACPA, Fluka) and phosphorus pentachloride (PCl<sub>5</sub>, Fluka) was dried in a vacuum over silica gel overnight before use. Triethylamine (TEA, Aldrich) was dried over magnesium sulfate (Riedel-de Haën), filtered, and distilled. The solvent 1,4-dioxane (Lab-Scan) used in polymerizations was freed from a stabilizer by distillation. Benzene (Merck), *n*-hexane (Lab-Scan), chloroform (Lab-Scan), and diethyl ether (Riedel-de Haën) were dried by conventional drying methods. Acetone (Rathburn) was used as received. The water used for all the measurements was purified and deionized in an Elgastat UHQ-PS purification system. The fluorescent probe 4-(dicyanomethylene)-2-methyl-6-(*p*-(dimethylamino)styryl)-4H-pyran (4HP, Aldrich) was used as received. The chemical structure of the probe is shown in Scheme 1.

**Syntheses.** Macroazoinitiators MAI<sub>550</sub> and MAI<sub>1900</sub>. The preparation of macroazoinitiators was conducted in two steps. In the first step, ACPA was converted to the corresponding acyl chloride, 4,4'-azobis(4-cyanopentanoyl chloride) (ACPC), by the method of Smith.<sup>18</sup> ACPA was treated with PCl<sub>5</sub> in a

**Table 1. Syntheses and Characteristics of PNIPA-*b*-PEOs**

sample	$n$ (NIPA), mmol	MAI <sub>1900</sub> , <sup>a</sup> mol %	MAI <sub>550</sub> , <sup>a</sup> mol %	solvent, mL	$M_n$ (PNIPA), <sup>b</sup> g mol <sup>-1</sup>	NIPA/EO <sup>c</sup>
NE-A	17.7	0.01		20	734 000	151
NE-B	17.7	0.1		20	334 000	69
NE-C	8.8	1.0		10	61 000	13
NE-1	17.7		0.01	20	345 000	244
NE-2	17.7		0.1	20	151 000	107
NE-3	8.8		1.0	10	39 000	27

<sup>a</sup> Concentrations of MAIs are shown as molar percentages of NIPA. <sup>b</sup> Determined by <sup>1</sup>H NMR. <sup>c</sup> Molar ratio of NIPA and EO repeating units in the blocks.

molar ratio of 1:2 in benzene at room temperature. In the second step, MAI was prepared by a condensation reaction of ACPC and PEO in dichloromethane in the presence of an excess amount of triethylamine for 24 h.<sup>19</sup> MAI<sub>550</sub> was purified from unreacted PEO and azoinitiator having only one PEO chain by dialysis (Spectro/Por, cutoff 1000) for 10 days at 5 °C. MAI<sub>1900</sub> was purified by ultrafiltration (Millipore, regenerated cellulose, membrane cutoff 10 000). The products were analyzed by <sup>1</sup>H NMR and SEC.

**PNIPA-*block*-PEOs.** Given amounts of NIPA and MAI (see Table 1) were dissolved in dioxane and flushed with nitrogen for 30 min at room temperature. Then the mixtures were heated to 65 °C and polymerized for 20 h. Next, the block copolymers were precipitated into diethyl ether. Reprecipitation was carried out in an acetone/diethyl ether mixture. The removal of residual MAI was conducted by centrifuging aqueous solutions (5000 rpm, Sigma 2K15C) at 50 °C. The centrifugation was repeated five times for 1 h at each. The complete removal of the unreacted PEO was ascertained by <sup>1</sup>H NMR. The separated polymers were dried in a vacuum. After this the polymers were once precipitated in an acetone/diethyl ether mixture and dried in a vacuum.

In the text, the copolymers containing PEO blocks with  $M_w$  550 or 1900 g/mol are simply called those with a short or a long PEO block, respectively. Block copolymers having an equal PEO block are called a copolymer set.

**Sample Preparation.** *Pure Aqueous Polymer Solutions.* The aqueous stock solutions of the block copolymers were prepared by dissolving the dry polymer in a known amount of water. In the present case, because the  $M_n$  of the PNIPA blocks were known, the polymer concentrations are given in moles of PNIPA blocks per liter. The samples were all diluted from the stock solutions.

*Samples with the Fluorescent Probe 4HP.* Samples 1: Aqueous polymer samples for light scattering and fluorescence measurements were prepared by first dissolving the copolymers and 4HP separately in chloroform. Known amounts of polymer solution and probe solution were carefully mixed, and the solvent was evaporated with a stream of air. Then, known volumes of deionized water were added on the thin films of polymer containing the probe. The solutions were kept in a refrigerator for 24 h for the complete dissolution of both the polymer and the probe. Samples 2: A known amount of 4HP dissolved in chloroform was placed into a vessel, and the solvent was evaporated. The aqueous copolymer solution with a fixed polymer concentration was added to the vessel containing 4HP. The solutions were kept in a refrigerator for 3 days in order to dissolve an equilibrium amount of 4HP in the polymer solution. Because of the poor water solubility of the probe, the concentration of the probe in the samples 2 was lower than in the samples 1. However, the equilibrium concentration of the probe in the former samples was not determined.

**Instrumentation and Characterization.** *NMR Spectroscopy.* <sup>1</sup>H NMR spectra of the block copolymers were measured with a 200 MHz Varian Gemini 2000 spectrometer using CDCl<sub>3</sub> as a solvent. The compositions of the block copolymers PNIPA-*b*-PEO were determined by <sup>1</sup>H NMR from the characteristic peaks of the repeating units. <sup>1</sup>H NMR (CDCl<sub>3</sub>) [200 MHz]  $\delta$  ppm: 4.00 (br, 1H, -NH-CH<sub>2</sub>-Me<sub>2</sub>) for NIPA and 3.66 (-CH<sub>2</sub>-, EO-homosequence) for PEO.

**Light Scattering.** Static light scattering (SLS) and dynamic light scattering (DLS) measurements were conducted with a Brookhaven Instruments BI-200SM goniometer and a BI-9000AT digital correlator. The light source was Lexel 85 argon laser (514.5 nm, power range 15–150 mW). In SLS, the angular dependence of the time-averaged scattering intensity ( $R_\theta$ ) was measured. When the polymer concentration approaches zero and the scattering angle,  $\theta$ , is small, the weight-average molar mass,  $M_w$ , is proportional to  $R_\theta/Kc$ :

$$\left[\frac{Kc}{R_\theta}\right]_{c \rightarrow 0} = \frac{1}{M_w} \left(1 + \frac{16\pi^2}{3\lambda^2} \langle R_g^2 \rangle_z \sin^2\left(\frac{\theta}{2}\right)\right) \quad (1)$$

Here,  $K = 4\pi^2 n^2 (dn/dc)^2 / (N_A \lambda_0^4)$  in which  $n$ ,  $dn/dc$ ,  $N_A$ , and  $\lambda_0$  are the refractive index of the solvent, the specific refractive index increment, Avogadro's constant, and the wavelength of light in a vacuum, respectively. The wavelength in a given medium is defined as  $\lambda = \lambda_0/n$ . The refractive index increments ( $dn/dc$ ) of the block copolymers were calculated using the equation<sup>20</sup>

$$dn/dc = w_A(dn/dc)_A + w_B(dn/dc)_B \quad (2)$$

in which  $w_A$  and  $w_B$  are the mass fractions of pure polymers PNIPAA and PEO and  $(dn/dc)_A$  and  $(dn/dc)_B$  their refractive index increments, respectively. The  $dn/dc$  values for PNIPAA-*g*-PEOs have been experimentally studied by various investigators.<sup>3,4</sup> A temperature dependence has been observed to be minimal, this justifying the use of eq 2. The time correlation functions measured by DLS were analyzed with a Laplace inversion program (CONTIN). The range of polymer concentrations was  $3.0 \times 10^{-8}$ – $7.5 \times 10^{-7}$  mol/L of the repeating units. The polymer solutions without the fluorescent probe (4 HP) were clarified by filtering through Millipore membranes (0.45  $\mu$ m pore size). The polymer solutions with the probe were clarified by centrifugation at 15 °C (5000 rpm, 2 h). Experiments were carried out in a temperature range from 20 to 45 °C. The samples were heated fast from ambient temperature by placing them into the goniometer where temperature was 45 °C. The samples were equilibrated at this temperature at least for 2 h.

**Fluorescence Spectroscopy.** Fluorescence spectra were recorded using a Spex Fluorolog 3 spectrofluorometer at right angles. The temperature of the water-jacketed cell holder was controlled by a programmable circulation bath. The samples with polymer concentration of  $3 \times 10^{-7}$  M of repeating units and probe concentration of  $3.3 \times 10^{-6}$  M were excited at 469 nm. The slit widths were set at 2.0 nm for both the excitation and the emission. In a 1 cm cell, the samples were heated slowly with the heating rate of 0.1 °C/min.

**Cloud Point Measurements.** Turbidimetric measurements were conducted with a Shimadzu UV-1601PC spectrophotometer at the wavelength of 550 nm. The samples with the polymer concentration of  $3 \times 10^{-7}$  M repeating units were heated slowly at the heating rate of 0.1 °C/min.

**Size Exclusion Chromatography.** SEC measurements were conducted with Waters equipment using a Waters 2410 refractive index detector. The eluent was 0.1 M aqueous NaNO<sub>3</sub>. PEO standards (Polymer Laboratories) were used for the calibration.

## Results and Discussion

**Syntheses of PNIPAA-*block*-PEOs.** PEOs in the synthesis of MAIs were very narrowly distributed (PDI < 1.2) which enabled the calculation of the number-average molar mass for each PNIPAA block from the <sup>1</sup>H NMR spectra. Table 1 shows the molecular weights of PNIPAA blocks and the molar ratio of the repeating units of PNIPAA to those of PEO.

When calculating the molar masses of the PNIPAA blocks, it was assumed that the polymers are diblock copolymers. This naturally is a simplification because

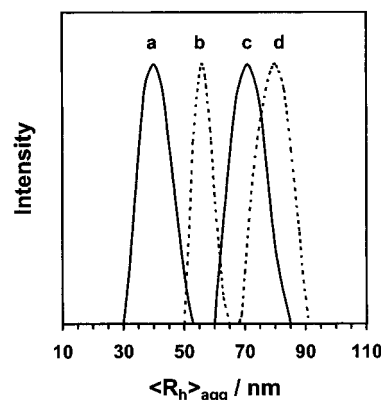


**Figure 1.** Size distributions of the aggregates in the aqueous NE-B solutions after fast heating to 45 °C. Polymer concentrations given in M PNIPAA blocks: (a)  $3.0 \times 10^{-8}$  M, (b)  $7.5 \times 10^{-8}$  M, (c)  $3.0 \times 10^{-7}$  M, and (d)  $7.5 \times 10^{-7}$  M.

it is well-known that radical polymerization may be terminated by the combination of two propagating chains. Also, the growing macroradical may react with the decomposed initiator.<sup>21</sup> These both reactions lead to triblock copolymers. The relative amounts of di- and triblock copolymers has not been studied, however, because the purpose of the present work is to find out how linear block copolymers differ from the graft copolymers recently investigated.<sup>4–6</sup> In addition, as often is the case with PNIPAA and its derivatives, repeatable size exclusion chromatograms are difficult to obtain.<sup>22</sup> In the present case, the retention time for all block copolymers was equal, regardless of molar mass.  $M_w/M_n$  from SEC varied from 1.5 to 1.6. However, the size distributions of the polymers in pure water by DLS at room temperature were monomodal. The average hydrodynamic radius ranged from 10 to 50 nm, and the polydispersity calculated by a second-order cumulant analysis ( $PD = \mu_2/\langle \Gamma \rangle^2$ ) varied from 0.21 to 0.24. This indicates that chain transfer reactions between PEO and growing macroradicals are not frequent, and the polymers are, at least mostly, linear.

**Cloud Points.** The cloud points of the aqueous polymer solutions were measured by following the changes in light transmitted through the sample. At the cloud point PNIPAA chains collapsed and formed aggregates. The critical temperatures of the samples NE-A, NE-B, and NE-C were 32, 33, and 34 °C, respectively. The increase in the cloud point was due to the decrease in the molar ratio NIPAA/EO. However, no change was observed with the block copolymers having the short PEO block: the cloud points were around 33 °C regardless of NIPAA/EO. The increase in the critical temperature with increasing content of PEO was also observed in our previous studies<sup>4</sup> with the graft copolymers of PNIPAA-*g*-PEO and in other studies with the block copolymers of PNIPAA-*b*-PEO.<sup>2,23</sup> Thus, the length of PEO block is of importance for the solubilizing of collapsing PNIPAA but has a minor effect on its cloud point.

**Light Scattering.** Above the critical temperature the block copolymers formed aggregates with narrow size distributions (see Figure 1). Polydispersities of the aggregates were  $PD = \mu_2/\langle \Gamma \rangle^2 \leq 0.1$ .

Figures 2 and 3 show the average hydrodynamic radii,  $\langle R_h \rangle_{agg}$ , and the apparent molecular weights,  $\langle M_w \rangle_{agg}$ , of the aggregates at 45 °C. Interestingly, the  $\langle M_w \rangle_{agg}$  increased linearly whereas  $\langle R_h \rangle_{agg}$  increased logarithmi-



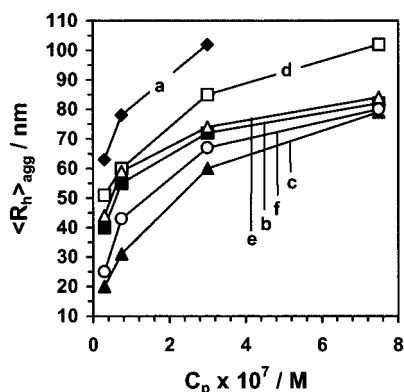


**Figure 2.** Average hydrodynamic radii of the aggregates,  $\langle R_h \rangle_{\text{agg}}$ , in the aqueous block copolymer solutions at different polymer concentrations,  $C_p$ , given in M PNIPA blocks, after fast heating to 45 °C: (a) NE-A, (b) NE-B, (c) NE-C, (d) NE-1, (e) NE-2, and (f) NE-3.

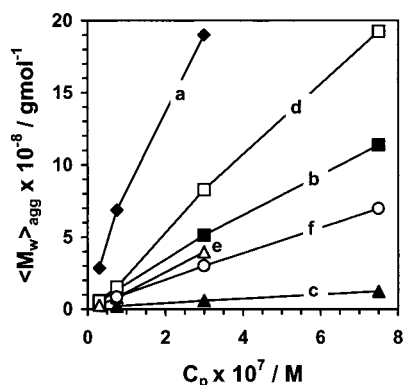


**Figure 3.** Apparent molecular weights of the aggregates,  $\langle M_w \rangle_{\text{agg}}$ , in the aqueous solutions at different polymer concentrations,  $C_p$  (in M PNIPA blocks), after fast heating to 45 °C: (a) NE-A, (b) NE-B, (c) NE-C, (d) NE-1, (e) NE-2, and (f) NE-3.

cally with increasing polymer concentration,  $C_p$ . This result was surprising since in our previous studies with PNIPA-*g*-PEO graft copolymers, both  $\langle M_w \rangle_{\text{agg}}$  and  $\langle R_h \rangle_{\text{agg}}$  showed logarithmic tendency as  $C_p$  varied.<sup>5</sup> It is assumed that different aggregation behavior is dependent on the structure of the block (a PEO chain attached at one or both ends of a PNIPA chain) and graft (several PEO chains randomly distributed along the PNIPA) copolymers. Within a copolymer set, i.e., either with a short or a long PEO block, the  $\langle R_h \rangle_{\text{agg}}$  values increased when the length of the PNIPA block (and NIPA/EO) increased. The aggregate size was more dependent on the molar ratio NIPA/EO than on the length of the PNIPA block when the  $\langle R_h \rangle_{\text{agg}}$  values were compared between two copolymer sets. The only exception was the copolymer with the longest PNIPA block which formed the biggest aggregates at every concentration. Within the both copolymer sets  $\langle M_w \rangle_{\text{agg}}$  also decreased when the PNIPA block shortened, i.e., NIPA/EO decreased. Also, the decrease of  $\langle M_w \rangle_{\text{agg}}$  generally followed the decreasing order of NIPA/EO within both copolymer sets. It is pointed out that upon dilution the  $\langle M_w \rangle_{\text{agg}}$  values of the samples approached more or less the same value. It is expected that a further dilution of the polymer solutions leads to a state at which  $\langle M_w \rangle_{\text{agg}}$  values of the different copolymer aggregates are the same, however, the number of chains being different. In addition, in extreme dilution the number of chains probably approaches the

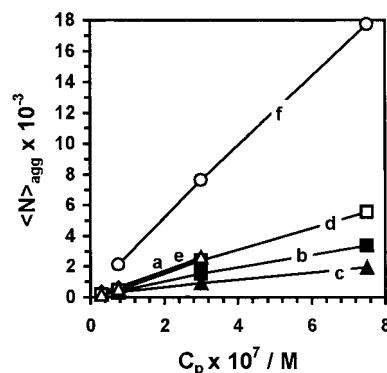


**Figure 4.** Average numbers of the polymer chains in the aggregates,  $\langle N \rangle_{\text{agg}}$ , at different polymer concentrations,  $C_p$  (in M PNIPA blocks), after fast heating to 45 °C: (a) NE-A, (b) NE-B, (c) NE-C, (d) NE-1, (e) NE-2, and (f) NE-3.

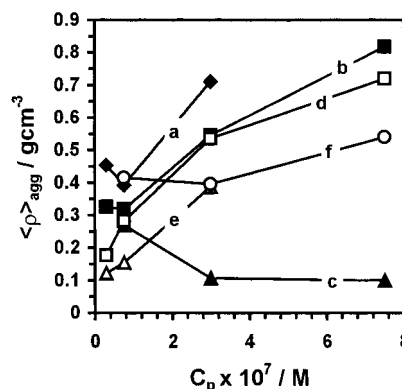


**Figure 5.** Average densities of the aggregates,  $\langle \rho \rangle_{\text{agg}}$ : (a) NE-A, (b) NE-B, (c) NE-C, (d) NE-1, (e) NE-2, and (f) NE-3.

value of unity. This dilute solutions could not be studied, however.

Figure 4 shows the average number of polymer chains in the aggregates,  $\langle N \rangle_{\text{agg}}$ , at 45 °C. As expected,  $\langle N \rangle_{\text{agg}}$  increased with  $C_p$ . However, an interesting difference was observed between the copolymer sets. The copolymers with the long PEO block showed a decreasing tendency in  $\langle N \rangle_{\text{agg}}$  with decreasing length of PNIPA block whereas the copolymers with the short PEO block showed an increasing tendency. This is understood by the steric stabilization of the aggregates by PEO to be more effective as the length of PEO block increases. A similar conclusion has been drawn for example concerning the micellization of PEO-*b*-poly(sodium methacrylate) block copolymer complexes in aqueous solutions.<sup>24</sup>

The average densities of the aggregates,  $\langle \rho \rangle_{\text{agg}}$ , at 45 °C were estimated by the equation  $\langle \rho \rangle = M_w / [(4/3)\pi \langle R_h \rangle^3 N_A]$ , where  $N_A$  is Avogadro's constant. Figure 5 shows that  $\langle \rho \rangle_{\text{agg}}$  generally increases with increasing  $C_p$ . Within a copolymer set the densities of the aggregates decreased as the length of PNIPA and the ratio NIPA/EO decreased. The samples NE-C and NE-3 having the lowest NIPA/EO ratios, however, behaved differently. This results from the high amount of PEO buried inside the core of the aggregate. This, especially in the case of NE-C, prevents the effective shrinkage of the core.

The ratio of the average radius of gyration to the average hydrodynamic radius,  $\langle R_g \rangle / \langle R_h \rangle$ , estimates the conformation of a polymer in solution. This ratio may be used in the present case as well, owing to the very narrow size distributions of the aggregate particles. As is seen in Figure 6, the conformations of the aggregates were strongly dependent on the polymer concentration

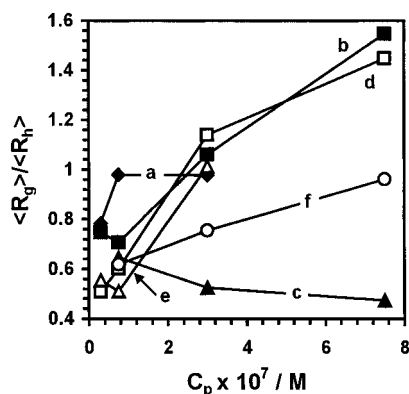


**Figure 6.** Ratio of the average radii of gyration to the average hydrodynamic radii of the aggregates,  $\langle R_g \rangle / \langle R_h \rangle$ : (a) NE-A, (b) NE-B, (c) NE-C, (d) NE-1, (e) NE-2, and (f) NE-3.

and NIPA/EO ratio. When lowering  $C_p$ , the structure of aggregates approached the  $\langle R_g \rangle / \langle R_h \rangle$  value of a globule, 0.78.<sup>25</sup> However, with the highest polymer concentration the  $\langle R_g \rangle / \langle R_h \rangle$  changed from around 1.5 (coillike structure)<sup>25</sup> to around 0.4 with decreasing the NIPA/EO ratio. The value 1.5 sometimes is indicative of the polydispersity of the sample. In the present case this does not apply, however, because all the size distributions were very narrow. One possible explanation is that with increasing polymer concentration the shape of the aggregates changes. Our suggestion is that the aggregates change from spherical to ellipsoidal. With high density of the core, PNIPA could form glassy domains<sup>26</sup> which may have an influence on the structure of aggregates as a whole. The block copolymer NE-C which had the lowest NIPA/EO ratio formed globular particles at every polymer concentration. More precisely,  $\langle R_g \rangle / \langle R_h \rangle$  values were even smaller than 0.78. This is explained by a higher chain density at the center than near the surface of the aggregate.<sup>3,27</sup>

**Comparison of NE-B and NE-1.** The block copolymers NE-B and NE-1 having approximately the same block length of PNIPA but the different block length of PEO showed different aggregation behavior upon heating. At each  $C_p$ , the copolymer with higher NIPA/EO ratio, NE-1, formed the aggregates whose  $\langle R_h \rangle_{\text{agg}}$ ,  $\langle M_w \rangle_{\text{agg}}$ , and  $\langle N \rangle_{\text{agg}}$  were larger than those of NE-B. No particular differences in the average densities and shape of the aggregates with  $C_p$  were observed. However, the core of the aggregate of NE-B (NIPA/EO = 69) was more heterogeneously packed than that of NE-1 (NIPA/EO = 244). Thus, the longer the PEO block is, the more effective is the solubilizing effect of PEO on the collapsing PNIPA to prevent further aggregation.

**Dilution of the Aggregates at 45 °C.** The aggregated solutions of NE-B and NE-1 with the highest polymer concentration were diluted with water, keeping the temperature constant at 45 °C. The diluted samples were equilibrated at least an hour, and  $\langle R_h \rangle_{\text{agg}}$  was remeasured. The purpose was to study whether the aggregates once formed decompose or not upon dilution. Figure 7 shows the  $\langle R_h \rangle_{\text{agg}}$  values of the diluted samples compared with the aggregate sizes of the corresponding samples shown in Figure 2. The sizes of the aggregates only slightly decreased with decreasing  $C_p$ . This was also the case in our similar measurements with PNIPA-*g*-PEO graft copolymers.<sup>28</sup> It seems that the aggregates once formed do not easily reorganize upon dilution, implying that polymer chains in the aggregate core are kinetically trapped.

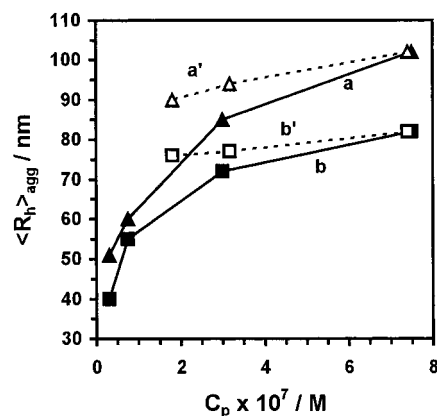


**Figure 7.** Average hydrodynamic radii of the aggregates,  $\langle R_h \rangle_{\text{agg}}$ , in the aqueous solutions at different polymer concentrations,  $C_p$  (in M PNIPA blocks), after fast heating to 45 °C: (a) NE-1 and (b) NE-B. The samples with  $C_p = 7.5 \times 10^{-7}$  M after dilution at 45 °C: (a') NE-1 and (b') NE-B.

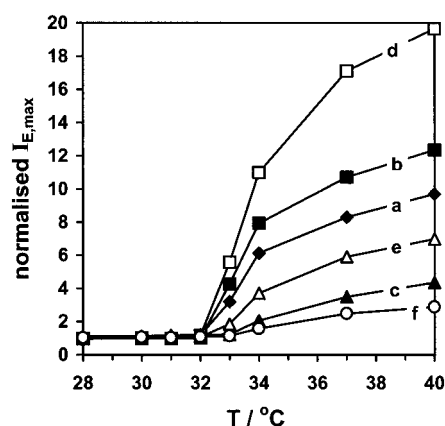


**Figure 8.** Normalized maxima of the emission intensities of the probe 4HP,  $I_{E, \text{max}}$ , in the aqueous block copolymer solutions during the slow heating of samples 1: (a) NE-A, (b) NE-B, (c) NE-C, (d) NE-1, (e) NE-2, and (f) NE-3. Polymer concentration  $3 \times 10^{-7}$  M of PNIPA blocks. Probe concentration  $3.3 \times 10^{-6}$  M.

**Fluorescence Spectroscopy.** First, the copolymer solutions containing the fluorescent probe 4HP were studied by light scattering. The method of preparing samples 1 resulted in aggregated solutions at room temperature whether the sample contained the probe or not. As was observed in our previous studies as well,<sup>6</sup> the aggregation is not solely due to the presence of the probe, but the method of the sample preparation plays an important role in the intercatenary binding of the polymers. Samples 2 showed no aggregation at room temperature, and their hydrodynamic radii were similar to the polymers without the probe. Both sample sets were heated slowly from room temperature to 40 °C. An increase in the emission intensity of the probe around the critical temperature of the samples indicated the collapse and phase separation of the PNIPA blocks. The critical temperatures of the samples were similar to the cloud points from turbidimetric measurements.

Figure 8 shows the normalized maxima of the emission intensities of the probe, i.e., normalized  $I_{E, \text{max}}$ , in samples 1 with increasing temperature. Within the copolymer set, the changes in microviscosity in the surroundings of the probe increased during the phase separation with the increasing length of PNIPA block. Again, the only exception was the copolymer with the longest PNIPA segment. Comparing the two copolymer

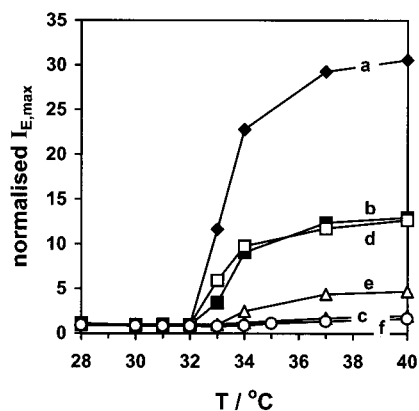


**Figure 9.** Normalized maxima of the emission intensities of the probe 4HP,  $I_{E,max}$ , in the aqueous block copolymer solutions during the slow heating of samples 2: (a) NE-A, (b) NE-B, (c) NE-C, (d) NE-1, (e) NE-2, and (f) NE-3. Polymer concentration  $3 \times 10^{-7}$  M of PNIPA blocks.

**Table 2. Wavelengths of the Maxima of the Emission Intensity of the Probe 4HP,  $\lambda_{max}$ , and the Difference of the  $\lambda_{max}$  Values before and after Heating the Aqueous Block Copolymer Samples 1**

sample	$\lambda_{max}/nm$		$\Delta\lambda_{max}/nm$ $\lambda_{max}(25\text{ }^{\circ}C) - \lambda_{max}(40\text{ }^{\circ}C)$
	25 °C	40 °C	
NE-A	580	608	-28
NE-B	609	608	1
NE-C	617	606	11
NE-1	615	607	8
NE-2	617	606	11
NE-3	628	611	17

sets, the changes in the microviscosity were more notable with the copolymers having the short PEO block.

During the collapse, the wavelength of the  $I_{E,max}$ ,  $\lambda_{max}$ , shifted, indicating changes in the polarity of the surroundings of the probe. Table 2 shows the  $\lambda_{max}$  values at 25 and 40 °C. At room temperature, within a copolymer set, the  $I_{E,max}$  occurred at shorter wavelengths as the length of PNIPA increased; i.e., the environment of the probe changed to a less hydrophilic one. If these two copolymer sets are compared, it is observed that the probe in the solutions of the copolymers having the short PEO block sensed more hydrophilic environment at room temperature than in the solutions with the long PEO block. However, after heating to 40 °C the probe sensed the same nonpolar environment regardless of the block copolymer.

Figure 9 shows the normalized  $I_{E,max}$  values for samples 2 as a function of temperature. Within the copolymer set the changes in the microviscosity of the probe during the collapse increased as the PNIPA block was lengthened. It seems that these changes are solely governed by the length of PNIPA block, not by the ratio NIPA/EO. Contrary to samples 1, these changes were more dramatic in the copolymers having the long PEO block. It was notable that the  $\lambda_{max}$  did not vary during the aggregation of the samples;  $\lambda_{max} \sim 611$  nm was more or less the same as the  $\lambda_{max}$  values for samples 1 at 40 °C.

**Localization of the Probe in Samples 1 and 2.** It is obvious that the localization of the probe around the block copolymer is dependent on the method of the sample preparation. That was also the case in our previous EPR studies with PNIPA-*g*-PEO graft copolymers.<sup>6</sup> Depending on the way of preparing the samples

a spin probe, 5-doxylstearic acid (5-DS), located either in the outer PEO shell of the copolymers or deeper inside, near the interface of PNIPA and PEO. The former and latter samples were prepared by using the preparation methods of samples 2 and 1, respectively, described in this paper. The fluorescent probe 4HP is more hydrophobic than 5-DS, and therefore, 4HP is most likely found in the hydrophobic domains of the block copolymers.

At 25 °C, in the aggregated samples 1 within a copolymer set the  $I_{E,max}$  shifted to a higher wavelength with decreasing block length of PNIPA. The increased polarity around the probe is understood by the increased amount of PEO and water inside the aggregates. The difference between the copolymer sets is explained by more effective phase separation between the PNIPA and PEO as the length of PEO block increases. Therefore, the changes in the microviscosity and the polarity around the probe decrease.

Samples 2 were not aggregated at room temperature. Thus, it should be stressed that during the heating of samples 2 the aggregates are assumed to form up in the same manner as of the samples without the probe. As already mentioned, the  $I_{E,max}$  values did not shift during the collapse of the PNIPA block but were more or less the same as the  $I_{E,max}$  values of samples 1 at 40 °C. According to these results, it is assumed that at room temperature the probe located in more homogeneous environment in samples 2 than in samples 1, the location of the probe being greatly influenced by the copolymer in the latter ones. At elevated temperatures, however, the probe resided in similar hydrophobic environments in all the samples.

**Comparison of NE-B and NE-1.** As discussed above, the extent of the phase separation between PNIPA and PEO in samples 1 was dependent on the block length of PEO. At room temperature, the aggregates of NE-B were more phase separated than those of NE-1, this leading to lower changes in microviscosity and polarity around the probe in the former aggregates. Interestingly, samples 2 of these two block copolymers showed no difference during heating. When these results are compared with the ones conducted by light scattering, one can notice that the average densities of the aggregates between the NE-B and NE-1 showed only a slight difference. Hence, it can be concluded that the size and the molecular weight of the aggregate are strongly dependent on the length of the PEO block. This emerges from the improved steric stabilization of the aggregates by the shell formed by the long PEO block. On the other hand, the hydrophobicity and density of the aggregate core, which consists of mainly PNIPA but also of some PEO, are not dependent on the length of PEO but on that of PNIPA. However, as discussed earlier, the polymer mass is differently distributed in the aggregate cores though approximately the same in the average.

## Conclusions

The syntheses of the block copolymers PNIPA-*b*-PEO were carried out by using different amounts of macroazoinitiators in the polymerization of NIPA. Two macroazoinitiators bearing PEO chains with different chain lengths were prepared via the reaction between an acyl chloride and the terminal hydroxyl groups of PEO.

The cloud points of the aqueous copolymer solutions were more dependent on the length of the PEO block



than on the molar ratio of the repeating units of PNIPA to those of PEO. The long PEO block shifted the LCST of the copolymers to higher temperatures as the NIPA/EO decreased, whereas this shift was not observed with the samples with the short PEO block.

Light scattering measurements showed that the aggregate formation and the structure of the aggregates in the aqueous block copolymer solutions at temperatures above the critical temperature were greatly dependent on the polymer concentration and the NIPA/EO ratio. At low polymer concentration and/or NIPA/EO the aggregates were spherical nanoparticles whose core consisted mainly of PNIPA and some PEO, stabilized by a PEO shell. When lowering the polymer concentration and/or NIPA/EO, the  $\langle M_w \rangle$  of the aggregates decreased faster than their hydrodynamic size. In some cases, the  $\langle R_g \rangle / \langle R_h \rangle$  of the aggregates was even lower than that typical for a spherical structure. Upon dilution and/or decreasing NIPA/EO the phase separation between the PNIPA and PEO blocks was enhanced. The solubilizing effect of PEO on the collapsing PNIPA was enhanced as well. All this resulted in aggregates with the inner part of the core denser than the rest of the aggregate. With increasing polymer concentration the shape of the aggregate was concluded to change from spherical to ellipsoidal. The mass distribution inside an aggregate became homogeneous while the density increased dramatically with increasing polymer concentration.

The fluorescent probe resided in different parts of the hydrophobic domains of the block copolymer, depending on the method of the sample preparation. The long PEO block enhanced the phase separation of PNIPA and PEO in the aggregated copolymer samples 1, which was observed as a blue shift in the  $I_{E,max}$  at room temperature. Samples 2, which were not aggregated at room temperature, showed no change in the wavelength of the  $I_{E,max}$  during the heating. The changes in the microviscosity of the surroundings of the probe increased with the length of the PNIPA block. At the collapsed state of the copolymer, however, the wavelengths of the  $I_{E,max}$  of the both sample sets were approximately the same, indicating the similar nonpolar environment around the probe independent of the block copolymer.

**Acknowledgment.** The work was supported by the Finnish Technology Agency (TEKES).

## References and Notes

- (1) (a) Tuzar, Z.; Kratochvil, P. In *Surface and Colloid Chemistry*; Matijevic, E., Ed.; Plenum Press: New York, 1993; Vol. 15, p 1. (b) Gao, Z.; Varshney, S. K.; Wong, S.; Eisenberg, A. *Macromolecules* **1994**, *27*, 7923. (c) Bo, G.; Wesslén, B.; Wesslén, K. B. *J. Polym. Sci., Part A: Polym. Chem.* **1992**, *30*, 1799. (d) Chiu, H.-C.; Chern, C.-S.; Lee, C.-K.; Chang, H.-F. *Polymer* **1998**, *39*, 1609. (e) Chen, M.-Q.; Kishida, A.; Seriwaza, T.; Akashi, M. *J. Polym. Sci., Part A: Polym. Chem.* **2000**, *38*, 1811.
- (2) Topp, M. D. C.; Dijkstra, P. J.; Talsma, H.; Feijen, J. *Macromolecules* **1997**, *30*, 8518.
- (3) Qiu, X.; Wu, C. *Macromolecules* **1997**, *30*, 7921.
- (4) Virtanen, J.; Baron, C.; Tenhu, H. *Macromolecules* **2000**, *33*, 336.
- (5) Virtanen, J.; Tenhu, H. *Macromolecules* **2000**, *33*, 5970.
- (6) Virtanen, J.; Lemmetyinen, H.; Tenhu, H. *Polymer* **2001**, *42*, 9487.
- (7) (a) Martin, T. J.; Prochazka, K.; Munk, P.; Webber, S. E. *Macromolecules* **1996**, *29*, 6071. (b) Bütün, V.; Billingham, N. C.; Armes, S. P. *J. Am. Chem. Soc.* **1998**, *120*, 11818.
- (8) (a) Wesslén, B. *Macromol. Symp.* **1998**, *130*, 403. (b) Kawauchi, S.; Winnik, M. A.; Ito, K. *Macromolecules* **1996**, *29*, 4465. (c) Chiu, H.; Chern, C.; Lee, C.; Chang, H. *Polymer* **1998**, *39*, 1609. (d) Talingting, M. R.; Munk, P.; Webber, S. E.; Tuzar, Z. *Macromolecules* **1999**, *32*, 1593. (e) Heitz, C.; Prud'homme, R. K.; Kohn, J. *Macromolecules* **1999**, *32*, 658. (f) Xu, B.; Li, L.; Yekta, A.; Masoumi, Z.; Kanagalingam, S.; Winnik, M. A.; Zhang, K.; Macdonald, P. M. *Langmuir* **1997**, *13*, 2447.
- (9) Jankova, K.; Chen, X.; Kops, J.; Batsberg, W. *Macromolecules* **1998**, *31*, 538.
- (10) (a) Harris, J. M.; Zalipsky, S., Eds.; *Poly(ethylene glycol) Chemistry and Biological Applications*; ACS Symposium Series 680; American Chemical Society: Washington, DC, 1997. (b) Uhrich, K. E.; Cannizzaro, S. M.; Langer, R. S.; Shakesheff, K. M. *Chem. Rev.* **1999**, *99*, 3181. (c) Bromberg, L. E.; Ron, E. S. *Adv. Drug Delivery Rev.* **1998**, *31*, 197.
- (11) (a) Hoffman, A. S. *Macromol. Symp.* **1996**, *98*, 645. (b) Zhu, P. W.; Napper, D. H. *Chem. Phys. Lett.* **1996**, *51*, 256. (c) Snowden, M. J.; Chowdhry, B. A.; Vincent, B.; Morris, G. E. *J. Chem. Soc., Faraday Trans.* **1996**, *92*, 5013. (d) Galaev, I. Y.; Mattiasson, B. *Enzyme Microb. Technol.* **1993**, *15*, 354.
- (12) (a) Sedlak, M.; Cölfen, H. *Macromol. Chem. Phys.* **2001**, *202*, 587. (b) Sidorov, S. N.; Bronstein, L. M.; Valetsky, P. M.; Hartmann, J.; Cölfen, H.; Schnablegger, H.; Antonietti, M. *J. Colloid Interface Sci.* **1999**, *212*, 197.
- (13) Lin, H.-H.; Cheng, Y.-L. *Macromolecules* **2001**, *34*, 3710. (b) Çakmak, İ. *Macromol. Rep.* **1995**, *A32*, 1113.
- (14) (a) Jaeger, W.; Wendler, U.; Lieske, A.; Bohrisch, J. *Langmuir* **1999**, *15*, 4026. (b) Jaeger, W.; Hahn, M.; Lieske, A.; Zimmermann, A. *Macromol. Symp.* **1996**, *111*, 95. (c) Lieske, A.; Jaeger, W. *Macromol. Chem. Phys.* **1998**, *199*, 255. (d) Takahashi, H.; Ueda, A.; Nagai, S. *J. Polym. Sci., Part A: Polym. Chem.* **1997**, *35*, 69. (e) Chang, T. C.; Chen, H. B.; Chen, Y. C.; Ho, S. Y. *J. Polym. Sci., Part A: Polym. Chem.* **1996**, *34*, 2613. (f) Holappa, S.; Shan, J.; Karesoja, M.; Tenhu, H., submitted to *Macromolecules*.
- (15) Moad, G.; Chiefari, J.; Chong, Y. K.; Krstina, J.; Mayadunne, R. T. A.; Postma, A.; Rizzardo, E.; Thang, S. H. *Polym. Int.* **2000**, *49*, 993.
- (16) (a) Yamazaki, A.; Song, J. M.; Winnik, F. M.; Brash, J. L. *Macromolecules* **1998**, *31*, 109. (b) Ringsdorf, H.; Simon, J.; Winnik, F. M. *Macromolecules* **1992**, *25*, 5353. (c) Winnik, F. M.; Davidson, A. R.; Hamer, G. K.; Kitano, H. *Macromolecules* **1992**, *25*, 1876. (d) Ringsdorf, H.; Venzmer, J.; Winnik, F. M. *Macromolecules* **1991**, *24*, 1678. (e) Chen, J.; Jiang, M.; Zhang, Y.; Zhou, H. *Macromolecules* **1999**, *32*, 4861. (f) Noda, T.; Morishima, Y. *Macromolecules* **1999**, *32*, 4631.
- (17) (a) Vatanparast, R.; Li, S.; Hakala, K.; Lemmetyinen, H. *Macromolecules* **2000**, *33*, 438. (b) Hakala, K.; Vatanparast, R.; Li, S.; Peinado, C.; Bosch, P.; Catalina, F.; Lemmetyinen, H. *Macromolecules* **2000**, *33*, 5954.
- (18) Smith, D. A. *Macromol. Chem.* **1967**, *103*, 301.
- (19) (a) Nagamune, T.; Ueda, A.; Nagai, S. *J. Appl. Polym. Sci.* **1996**, *62*, 359. (b) Cvetkovska, M.; Lazarevic, M.; Koseva, S.; Baysal, B.; Hamurcu, E. E.; Uyanik, N. *J. Appl. Polym. Sci.* **1997**, *65*, 2173.
- (20) Zhou, Z.; Chu, B.; Peiffer, D. G. *Macromolecules* **1993**, *26*, 1876.
- (21) Odian, G. *Principles of Polymerization*, 3rd ed.; John Wiley & Sons: New York, 1991.
- (22) Ganachaud, F.; Monteiro, M. J.; Gilbert, R. G.; Dourges, M.-A.; Thang, S. H.; Rizzardo, E. *Macromolecules* **2000**, *33*, 6738.
- (23) Lee, K. K.; Jung, J. C.; Jhon, M. S. *Polym. Bull. (Berlin)* **1998**, *40*, 461.
- (24) Bronich, T. K.; Popov, A. M.; Eisenberg, A.; Kabanov, V. A.; Kabanov, A. V. *Langmuir* **2000**, *16*, 481.
- (25) Burckhard, W. *Adv. Polym. Sci.* **1998**, *143*, 173.
- (26) Afroze, F.; Nies, E.; Berghmans, H. *J. Mol. Struct.* **2000**, *554*, 55.
- (27) Wu, C.; Zhou, S. Q. *Macromolecules* **1995**, *28*, 8381.
- (28) Unpublished results.